Available online at www.sciencedirect.com
ScienceDirect
European Journal of Pharmaceutics and Biopharmaceutics 68 (2008) 535–544
European Journal of Pharmaceutics and Biopharmaceutics
www.elsevier.com/locate/ejpb

Research paper

Cyclosporine-loaded solid lipid nanoparticles (SLN®): Drug–lipid physicochemical interactions and characterization of drug incorporation

R.H. Müller [a], S.A. Runge [a], V. Ravelli [b], A.F. Thünemann [c], W. Mehnert [a], E.B. Souto [a,d,*]

[a] Department of Pharmaceutics, Biopharmaceutics and Biotechnology, Free University of Berlin, Berlin, Germany
[b] Institute of Nanosurgery, University of Pisa, Italy
[c] Division of Structure Analysis, Federal Institute for Materials Research and Testing, Berlin, Germany
[d] Fernando Pessoa University, Department of Pharmaceutical Technology, Porto, Portugal

Received 4 February 2007; accepted in revised form 5 July 2007
Available online 17 July 2007

Abstract

Solid lipid nanoparticles (SLN) were produced loaded with cyclosporine A in order to develop an improved oral formulation. In this study, the particles were characterized with regard to the structure of the lipid particle matrix, being a determining factor for mode of drug incorporation and drug release. Differential scanning calorimetry (DSC) and wide-angle X-ray scattering (WAXS) measurements were employed for the analysis of the polymorphic modifications and mode of drug incorporation. Particles were produced using Imwitor®900 as lipid matrix (the suspension consisted of 10% particles, 8% Imwitor®900, 2% cyclosporine A), 2.5% Tagat S, 0.5% sodium cholate and 87% water. DSC and WAXS were used to analyse bulk lipid, bulk drug, drug incorporated in the bulk and unloaded and drug-loaded SLN dispersions. The processing of the bulk lipid into nanoparticles was accompanied by a polymorphic transformation from the β to the α-modification. After production, the drug-free SLN dispersions converted back to β-modification, while the drug-loaded SLN stayed primarily in α-modification. After incorporation of cyclosporine A into SLN, the peptide lost its crystalline character. Based on WAXS data, it could be concluded that cyclosporine is molecularly dispersed in between the fatty acid chains of the liquid-crystalline α-modification fraction of the loaded SLN.

Keywords: Solid lipid nanoparticles; Cyclosporine A; Characterization; Oral bioavailability; Lipid polymorphism

1. Introduction

Lipid nanoparticles with a solid matrix, such as solid lipid nanoparticles (SLN™), are an alternative nanoparticulate carrier system to polymeric nanoparticles, liposomes and o/w emulsions [1–4]. Aqueous SLN dispersions are composed of a lipid which is solid both at body and room temperature, being stabilized by a suitable surfactant. With regard to developing commercial products for the patient, SLN possess distinct advantages compared to other carriers, e.g., polymeric nanoparticles. Especially for topical and oral administration, all lipids can be used as matrix material, which are currently in use for creams, ointments, tablets, and capsule formulations including the long list of different surfactants/stabilizers employed in these traditional formulations. Thus, there is no problem with the regulatory accepted status of excipients [5–7].

For the production of SLN, different methods can be used such as high pressure homogenization [3,6,8–10], microemulsion technology [11–13], solvent evaporation [14,15] and solvent diffusion methods [16,17]. Large industrial scale production – a fundamental prerequisite for introducing a product to the market – is easily possible

* Corresponding author. Department of Pharmaceutics, Biopharmaceutics and Biotechnology, Free University of Berlin, Kelchstr. 31, D-12169 Berlin, Germany. Tel.: +49 30 83850678; fax: +49 30 83850616.
E-mail address: mpharma@zedat.fu-berlin.de (E.B. Souto).

0939-6411/$ - see front matter © 2007 Elsevier B.V. All rights reserved.
doi:10.1016/j.ejpb.2007.07.006

when employing high pressure homogenization [18,19]. Existing industrial production lines used for the production of parenteral o/w emulsions can also be used for lipid nanoparticle production [4]. These production lines are temperature controlled, which is required for production of the lipid nanoparticles at elevated temperature. The aqueous lipid nanoparticle dispersions can be transferred to dry oral dosage forms, e.g., pellets [20]. As in any solid particulate carrier, the release of drugs from lipid nanoparticles can be modulated in order to optimize their blood levels [21]. These features together make lipid nanoparticles an interesting carrier system for optimized oral delivery of drugs.

In this study, SLN were chosen to develop an optimized formulation for cyclosporine (CycA), intended for oral administration of this protein. The low oral bioavailability of CycA is due to its low solubility in water (0.02 mg/ml at 25 °C [22]) and additionally it is a substrate of P-glycoprotein [23]. To increase the solubility and subsequently improve absorption, CycA was administered orally dissolved in a mixture of corn oil and ethanol in the product Sandimmun® capsules [24,25]. This formulation shows pronounced variations in bioavailability from 10% to 60%, due to differences in the dispersion of the oil in the gut, to more or less finely dispersed oil droplets. The bioavailability was highly dependent on the emulsifying compounds in the gut, i.e., bile salts [24]. The second generation product Sandimmun® microemulsion avoided this problem. After dilution with water in the stomach the microemulsion breaks, i.e., it transforms to an ultrafine o/w emulsion thus eliminating the problem of mechanical dispersion. However, because emulsions do not provide the possibility of prolonged release, an initial plasma peak above 1000 ng/ml occurs. This peak is highly responsible for potential nephrotoxicity [25]. To obtain the same reproducible blood profile as the microemulsion, a new approach is the administration of an ultrafine lipid dispersion (aqueous SLN dispersion), possessing simultaneously controlled release properties due to a solid matrix.

The first step of developing such carrier systems is the preparation of an aqueous SLN dispersion with a sufficiently high loading capacity for CycA. Considering the single doses of 100–200 mg, the loading capacity calculated on the particle mass (lipid + CycA) should be 20% to keep the volume of the final oral formulation (tablet) within an acceptable range. Imwitor®900 was identified as lipid matrix showing sufficient incorporation capability. In previous studies the entrapment efficiency of CycA within these SLN was found to be 96.1% [26].

Drugs can be incorporated differently into the lipid matrix, e.g., molecularly dispersed (solid solution) [27] or in form of amorphous clusters or definite particles, e.g., magnetites [28]. In case of a solid solution, theoretically drugs can be localized in between fatty acid chains or the lamellae of the lipids. This paper investigates the mode of incorporation of CycA into the SLN for better understanding of the delivery system.

2. Materials and methods

2.1. Materials

Cyclosporine (CycA) was a gift from the company Pharmatec (Milan, Italy). The solid lipid Imwitor®900 (glycerol monostearate 40–50%) was purchased from Cognis (Dusseldorf, Germany). The emulsifiers Tagat®S (polyoxyethylene glycerol monosteatate) and sodium cholate were obtained from Goldschmidt (Essen, Germany) and Sigma (Deisenhofen, Germany), respectively. Water was collected by the MilliQ system Millipore (Schwalbach, Germany).

2.2. Methods

To access the maximum loading capacity of SLN for CycA physical mixtures composed solely of drug and lipid have been prepared by melting the Imwitor®900 and adding from 5% up to a maximum of 30% of peptide. These mixtures have been further analysed by differential scanning calorimetry (DSC) and wide-angle X-ray scattering (WAXS).

For the preparation of CycA-loaded SLN dispersions, a lipid phase composed of 2.0% (*m*/*m*) of drug and 8.0% (*m*/*m*) of Imwitor®900 was melted at approximately 5–10 °C above the melting point of the lipid (56–61 °C). The obtained melted phase was dispersed in an aqueous surfactant solution containing 2.5% (*m*/*m*) Tagat®S and 0.5% (*m*/*m*) sodium cholate heated at the same temperature. The final formulation contained consequently 87% water, 10% lipid phase (8% lipid plus 2% drug) and 3% surfactant mixture. The dispersion was performed by high speed stirring using an Ultra-Turrax (Jahnke & Kunkel, Staufen, Germany) for 1 min at 8000 rpm. The obtained pre-emulsion was homogenized at the temperature of the melt using a Micron LAB 40 (APV Homogenizers, Unna, Germany) applying 500 bar and three homogenization cycles.

Photon correlation spectroscopy (PCS), performed using a Zetasizer IV (Malvern Instruments, Malvern, United Kingdom), was used to assess the mean particle size (*z*-Ave, *z*-average) and the polydispersity index (PI). Laser diffractometry (LD) was employed to measure larger sized particles, i.e., outside the measuring range of PCS (>3 μm) using a Coulter LS 230 (Beckmann Coulter Counter, Kiel, Germany).

Differential scanning calorimetry (DSC) analysis was performed by a Mettler DSC 821^e (Mettler Toledo, Gießen, Germany). DSC scans were recorded at a heating and cooling rate of 5 K/min. The samples were weighted in 40 μl aluminium pans and heated from 20 °C up to 85 °C, kept for 15 min at 85 °C, cooled down to 20 °C, kept at 20 °C for 16 min, reheated again up to 150 °C and cooled down again to 20 °C.

Wide-angle X-ray scattering (WAXS) measurements were carried out with a Nonius PDS120 powder diffractometer by transmission geometry. A FR590 generator was used as the source for Cu K_α radiation ($\lambda = 0.15418$ nm),

monochromatization of the primary beam was achieved by means of a curved Ge crystal and the scattered radiation was measured with a Nonius CPS120 position sensitive detector. The resolution of this detector in 2θ was 0.018°, being the scattering vector defined as $s = (2/\lambda)\ \sin\theta$.

3. Results and discussion

3.1. Characterization of bulk lipid and drug

An important parameter affecting drug incorporation is the polymorphic modification of the lipid particle matrix. In general, the production process of the nanoparticles can change the type of modification of their respective fraction. The bulk lipid Imwitor®900 was analysed by DSC (Fig. 1). Table 1 shows the corresponding DSC data.

The first heating curve revealed an onset temperature of 58.1 °C, corresponding to the β′-modification of Imwitor®900 [29]. To produce SLN, the lipid is melted, the drug dissolved in the melted lipid and then this drug-containing melt is dispersed in a hot surfactant solution to yield a pre-emulsion. This pre-emulsion is homogenized to obtain a hot o/w nanoemulsion. Cooling leads to crystallization of the lipid and formation of SLN. This process means that, when analysing the SLN by DSC, the lipid has been melted before (drug dissolution process), i.e., DSC analysis of the SLN is a second melting process. Therefore, the bulk Imwitor®900 was heated a second time in the DSC (Fig. 1). The onset temperature was reduced from 58.1 °C to 53.4 °C corresponding to the α-modification of Imwitor®900 [30]. The melting enthalpy of the second heating curve is reduced, partially attributed to the fact that after 16 min of isotherm phase at 20 °C obviously the lipid was not yet fully crystallized. Little difference was seen between the two cooling curves (B and D, Fig. 1).

The DSC analysis of CycA revealed a melting with a maximum at 117 °C and an onset around 110 °C when applying a heating rate of 5 K/min (Fig. 2). The heat flow is less than 1 mW. Characteristic melts for CycA are reported at 190 °C for an orthorhombic crystal form and around 110 °C for a tetragonal form [31]. Therefore, the DSC trace is indicative for CycA present in a partial tetragonal crystalline form. The melting transition was broadened and shifted in the range 130–150 °C when applying a high heating rate of 25 K/min as expected. But surprisingly no melt was found in the second heating curve. The CycA is obviously not able to crystallize at this high cooling rate. It may be then either frozen in a liquid-like state (amorphous) or frozen in a thermotropic liquid-crystal state as it was reported for spray-dried CycA [31].

In the next development step of the SLN preparation physical mixtures of CycA and lipid were prepared containing 5% up to a maximum of 30% of drug. Bulk Imwitor®900 was used as reference. Based on the production process, the physical mixtures were heated to 85 °C to give CycA the possibility to dissolve to its maximum solubility, then the mixtures were cooled in order to re-crystallize. This procedure imitates the production process of the SLN. Then the mixtures were heated a second time. This heating curve corresponds now to the heating of the produced SLN. DSC analytical parameters were identical to the ones in Fig. 1. As shown in Fig. 1, after first heating the bulk Imwitor®900 transfers to the α-modification (Fig. 3). Distortion of the crystal lattice of Imwitor®900 increases with increasing CycA concentration leading to a reduction of onset temperature and melting peak. The decrease in these two temperatures indicates that CycA is obviously dissolved at each concentration. Note that CycA concentration is 20% (*m*/*m*) and higher

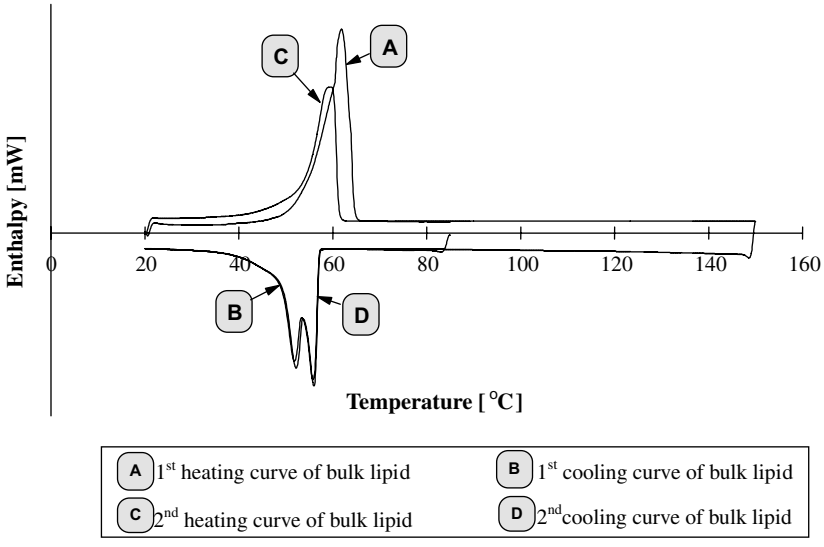

Fig. 1. DSC thermogram of bulk Imwitor®900. The sample was heated twice (A and C) and twice cooled (B and D). Heating and cooling rates were 5 K/min. The profile was: first heating phase 20–85 °C, 15 min isotherm at 85 °C, first cooling phase 85–20 °C, 16 min isotherm at 20 °C, second heating phase 20–150 °C, second cooling phase 150–20 °C.

Table 1
Onset temperature, melting point (=peak maximum) and melting enthalpy of Imwitor®900 bulk material from Fig. 1

DSC parameters	First heating curve	Second heating curve	First cooling curve	Second cooling curve
Onset temperature (°C)	58.1	53.4	57.2	57.2
Peak maximum (°C)	61.1	59.2	56.5/52.4	56.3/52.2
Melting enthalpy (J/g)	164.3	121.0	−120.6	−119.7

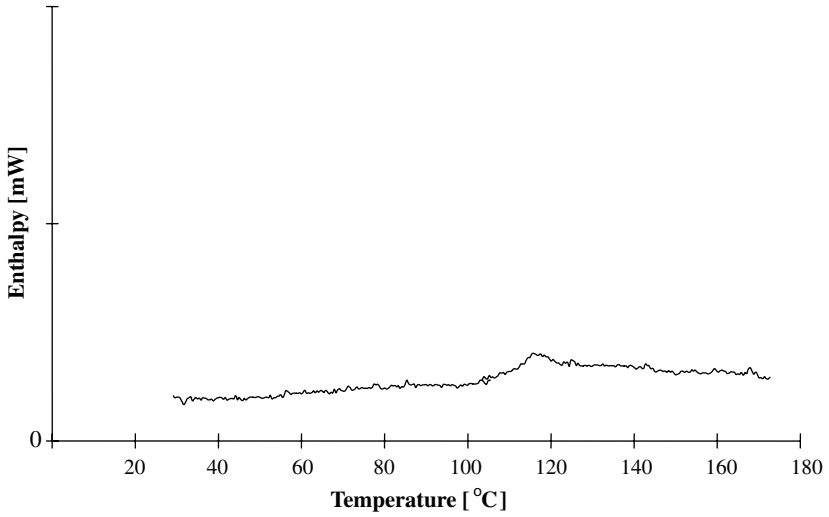

Fig. 2. DSC analysis of bulk CycA applying a heating rate of 5 K/min from 25 °C to 200 °C.

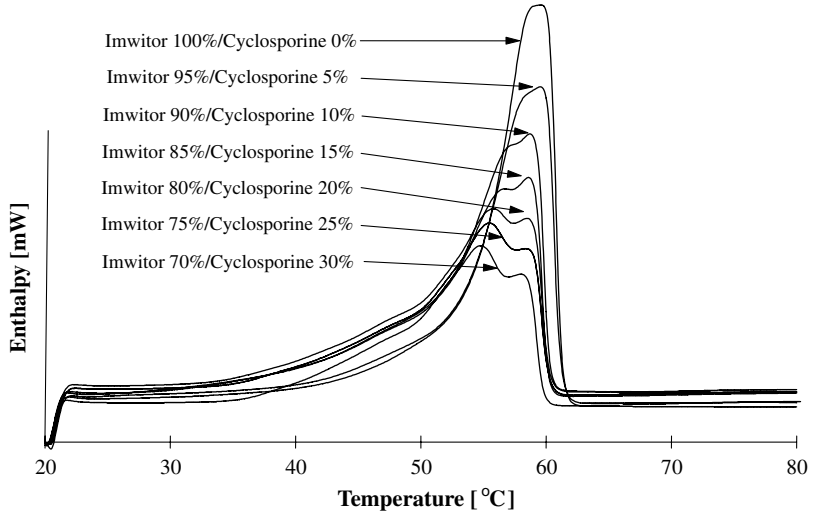

Fig. 3. DSC analysis (second heating curves) of mixtures of lipid with increasing CycA content from 5% to 30%. Bulk Imwitor®900 was used as reference. DSC analytical parameters were identical to Fig. 1.

amounts will lead to the formation of a second melting peak at 53.4 °C (Fig. 3). A potential explanation is an inhomogeneous drug distribution in the lipid matrix due to formation of domains containing different amounts of CycA. Table 2 shows the calculated data. The measured melting enthalpy was not related to the total weight of the sample but to the weight of the lipid (i.e., in case the sample contained 10% CycA, the melting enthalpy was calculated relating to 90% lipid in the sample).

The calculated melting enthalpy of the lipid fraction in the mixtures (116.7–119.0 J/g) shows little difference to the melting enthalpy of the bulk Imwitor®900 (121.0 J/g). Based on this, all mixtures are preferentially in the α-modification with an onset temperature ⩽53.4 °C. Drug concentrations above 20% lead to a further reduction of the onset temperature. Taking into account that the lipid particle matrix should be definitively in the solid state around body temperature, it was decided to take a loading of 20% CycA for preparing the drug-loaded SLN.

Table 2
Onset temperature, melting point (=peak maximum) and melting enthalpy of the second heating curves of lipid–CycA mixtures with increasing drug content from 0% to 30% (enthalpy calculated related to the total particle mass)

DSC parameters	0%	5%	10%	15%	20%	25%	30%
Onset temperature (°C)	53.4	52.1	49.7	49.3	48.1	47.1	45.2
Peak maximum (°C)	59.2	59.2	58.4	58.4	56.3	55.3	54.5
Melting enthalpy (J/g)	121.0	118.9	117.4	119.1	121.5	117.9	116.7

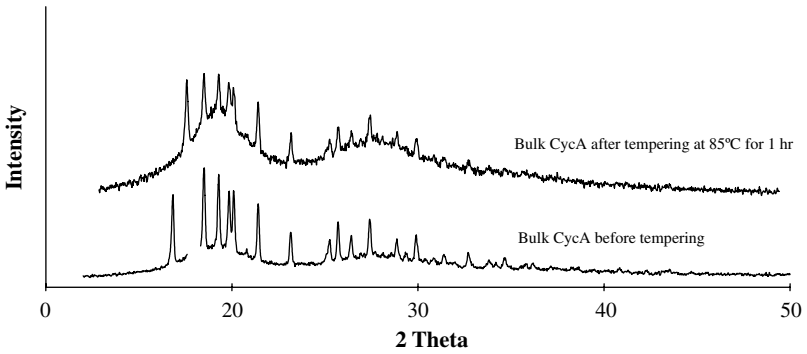

Fig. 4. WAXS analysis of CycA before (lower) and after (upper) tempering at 85 °C for 1 h. The incubation process at 85 °C resembles the heating process of CycA for dissolution in the melted lipid during the SLN production process.

3.2. X-ray analysis of bulk lipid and drug

Fig. 4 shows the WAXS diagram of CycA before and after tempering at 85 °C for 1 h. Maintaining CycA at 85 °C should imitate the heating procedure during the production of the SLN. To make potential changes more easily detectable, a heat exposure period of 1 h was selected being approximately five times longer than the heat exposure during the production process. CycA showed two broad reflections with maxima at 7° and 17°, respectively, which are typical for the frozen thermotropic liquid-crystal form of CycA [31] (Fig. 4, lower). In addition, the diagram shows sharp reflections with positions and intensity ratios that are consistent with the tetragonal crystal form of CycA [31]. Tempering for 1 h reduces the crystalline fraction in the CycA, the peaks are less pronounced and the intensity of the broad reflections increases corresponding to an increasing amount of CycA in its liquid-crystalline form (Fig. 4, upper).

WAXS analysis was employed to investigate the lamellae arrangement of the lipid molecules and the crystallinity of the fatty acid chains in the acylglycerols of Imwitor®900 (palmitic and stearic acids). Imwitor®900 is a mixture of mono-, di- and triacylglycerols. Due to the differences in the chain length of the two fatty acids and three hydroxyl groups of glycerol, formation of β′-modification takes place. WAXS analysis of Imwitor®900 was performed without pre-treatment (Fig. 5, lower) and after tempering the lipid at 85 °C for 1 h (Fig. 5, middle). This imitates heating of the lipid for dissolution of CycA during the SLN production process. Analysis was performed after storage of the tempered lipid for 24 h. Finally, the physical mixture of 80% Imwitor®900 and 20% CycA was melted at 85 °C to dissolve the CycA in the lipid. The mixture was re-crystallized and analysed after 24 h storage at room temperature (Fig. 5, upper). The detected scattering intensity was plotted as a function of the scattering vector s (positions of the maxima, marked in Fig. 5, are given in Tables 3 and 4).

The periodic arrangement of the lipid lamellae leads to equidistant maxima of the scattering vectors in the range from $s = 0.18\ \mathrm{nm}^{-1}$ to $1.00\ \mathrm{nm}^{-1}$. The scattering pattern in the range $2–3\ \mathrm{nm}^{-1}$ allows conclusions regarding the arrangement of the alkyl chains. Crystalline side chains in β-modification of Imwitor®900 lead to multiple scattering reflexes, the liquid-crystalline α-modification creates only a single scattering reflex [18].

Fig. 5 clearly shows the differences between the bulk Imwitor®900 before and after incubation at 85 °C and incorporation of 20% CycA, respectively. The distance of the lipid lamellae can be calculated from the peaks *1 to *4. The scattering peaks around peak *5 allow the identification of the modification. The lipid modification can be identified based on three criteria of the X-ray diffraction patterns when plotting the intensity versus the scattering vector s [32]:

1. A modification with a single scattering reflex of the lipid side chains of the glycerol at a Bragg distance of 0.415 nm is called α-modification.
2. A modification with two reflexes at Bragg distances of 0.389 nm and 0.420 nm is called β′-modification.
3. A modification which does not fulfil the above criteria is called β-modification.

Table 3 lists the reflex positions and the corresponding Bragg spacings from Fig. 5. All three samples display equidistance peaks *1–*4 indicating a lamellae structure. Tem-

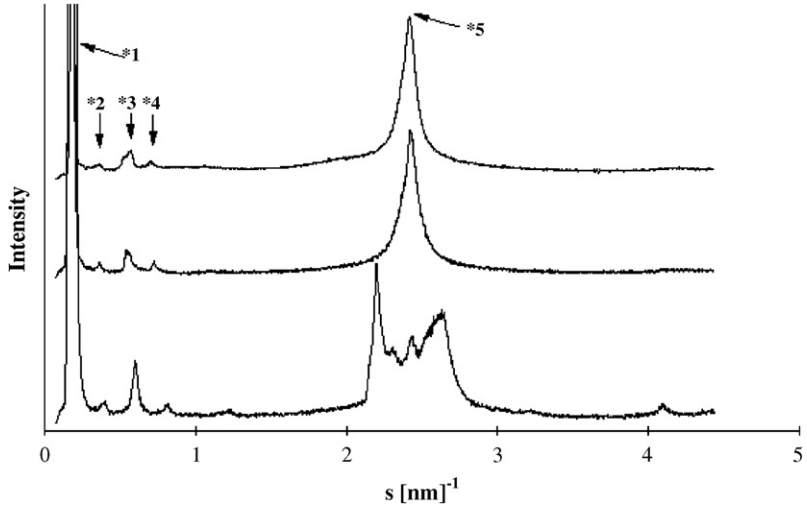

Fig. 5. WAXS diagrams of the bulk Imwitor®900 before tempering (β′-modification, lower), tempered Imwitor®900 for 1 h at 85 °C and analysed after 24 h storage at room temperature (α-modification, middle), and of Imwitor®900 loaded with 20% CycA by dissolving the drug in the melted lipid matrix at 85 °C, analysed after 24 h storage at room temperature (α-modification, upper) (*1–*4 – detection of periodic structures of the lipid lamellae; *5 – scattering peak range to identify the lipid modification).

Table 3
Position of the reflex maxima (*1–*4) and Bragg spacings (*d*) from Fig. 5, i.e., bulk lipid Imwitor®900 before tempering, after tempering Imwitor®900 for 1 h at 85 °C, and of 20% CycA-loaded Imwitor®900

Parameters	*1	*2 (≈2× *1)	*3 (≈3× *1)	*4 (≈4× *1)	*5
	Imwitor 900 before tempering				
s_{max} [nm^{-1}]	0.195	0.400	0.600	0.810	2.20/2.30 2.40/2.60
Bragg spacings [nm]	5.13	5.13	5.13	5.13	0.45/0.44 0.42/0.38
	Imwitor 900 after tempering				
s_{max} [nm^{-1}]	0.183	0.360	0.550	0.720	2.42
Bragg spacings [nm]	5.46	5.46	5.46	5.46	0.413
	Imwitor 900 containing 20% cyclosporine A				
s_{max} [nm^{-1}]	0.183	0.360	0.570	0.720	2.42
Bragg spacings [nm]	5.46	5.46	5.46	5.46	0.413

Table 4
Summary of crystallinity characteristics from Fig. 5

Imwitor®900	Before tempering	After tempering	Containing 20% CycA
Bragg spacing [nm]	5.13	5.46	5.46
Crystalline system	β′-modification (highly crystalline)	α-modification (less crystalline)	α-modification (less crystalline)

pering of the lipid, or incorporation of CycA in the lipid (Fig. 5, middle and upper), leads to an increase of the long period by 0.3 nm and a drastic decrease in side chain crystallinity. The increase in the long period of the lipid matrix from 0.514 nm to 0.546 nm (*1) indicates a lower ordering of the lamellar structure.

As shown by the *d* of the bulk Imwitor®900 in Table 3 (*5), the detection of sharp reflections in the range of $s = 2$ nm^{-1} to 3 nm^{-1} correspond to a high side chain crystallinity (after Hernqvist β- or β′-modification). Tempering of Imwitor®900 or incorporation of CycA leads to a reduced crystallinity of the side chains proven by the detection of a single scattering peak at $d = 4.13$ Å (ideally after Hernqvist being 0.415 nm). The lipid is in α-modification, the fatty acid chains can rotate around their axis. The intermolecular order between the fatty acid chains is very low (liquid-like). Table 4 summarizes the crystallinity criteria deduced from Fig. 5. In general, it can be concluded that the X-ray data confirm the modifications as determined on the basis of melting temperature and melting enthalpy from DSC analysis.

The *d* increased after tempering of the bulk lipid and also after incorporation of CycA into the bulk lipid. However, there is no difference in the lamellar spacings between

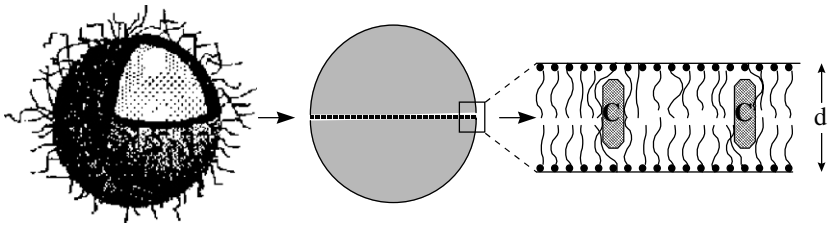

Fig. 6. Model of CycA incorporation in Imwitor®900: incorporation in between the fatty acid chains in parallel direction, no localization in between the lipid lamellae (structure derived from bulk lipid).

tempered lipid and CycA-loaded lipid. Based on this, the drug can only be incorporated in between the fatty acid chains of the α-modification of the lipid. A d of 0.546 nm allows theoretically incorporation of the CycA molecule parallel to the fatty acid chain. The size of the CycA molecule can be derived from the crystal data published by Hassan and Al-Yahya [33], considering the volume of the drug crystal of 1.974 nm^3, a tetragonal system with side lengths of $a = b \approx 0.87$ nm and $c \approx 2.61$ nm can be derived. Considering the length of the molecule, CycA can be easily incorporated in the fatty acid side chains of the lipid lamellae, which has a long period of 5.46 nm.

A phase separation in domains of CycA and domains of Imwitor®900 can be excluded. Such phase separation would have let to the detection of CycA crystal peaks. However, after incorporation of 20% CycA in Imwitor®900 no crystalline peaks were detected (Fig. 5, upper) as can be clearly seen in the scattering of the partially crystalline CycA (Fig. 4, lower and upper). Consequently, CycA is molecularly dissolved in the lipid matrix and does not re-crystallize after cooling of the CycA-Imwitor blend. Based on these assumptions, the model of CycA incorporation into SLN was developed as shown in Fig. 6.

3.3. Characterization of drug-free SLN dispersions

The drug-free SLN had a z-Ave diameter of 143 nm, PI of 0.220 and a LD diameter 95% of 0.790 μm. The production of SLN from bulk lipid can cause a change in the lipid modification. As already shown for the bulk lipid, the heating process can lead to a higher energy modification, in this case α-modification. The size of the lipid matrix can also affect the crystallization process. For example, it is known that very small melted lipid droplets show a delay in recrystallization. Very often they form supercooled melts [27,34,35]. Such lipid particle dispersion exhibiting a supercooled melt at room temperature can be transferred to a crystalline structure by reducing the temperature, e.g., replacing the suspension in the fridge. The melting temperature of the lipid is also affected by the particle size. A melting point reduction occurs according to the Thompson equation [36]. In order to differentiate between the actual effect of the SLN production process and the effect of the CycA, first drug-free aqueous SLN dispersions were prepared. The composition was 10% Imwitor®900, 2.5% Tagat®S, 0.5% sodium cholate and water.

From the DSC analysis of the bulk Imwitor®900 and of the aqueous 10% drug-free SLN suspension, the onset temperature was reduced from 58.1 °C (bulk) to 51.1 °C, the peak temperature from 61.1 °C to 57.5 °C and the calculated melting enthalpies from 164.3 J/g (bulk) to only 90.6 J/g. These results indicate that the lipid changed from β′-modification in the bulk, to the α-modification in the SLN (data not shown).

Fig. 7 shows the X-ray diffraction patterns of the drug-free SLN dispersion versus bulk Imwitor®900. The bulk

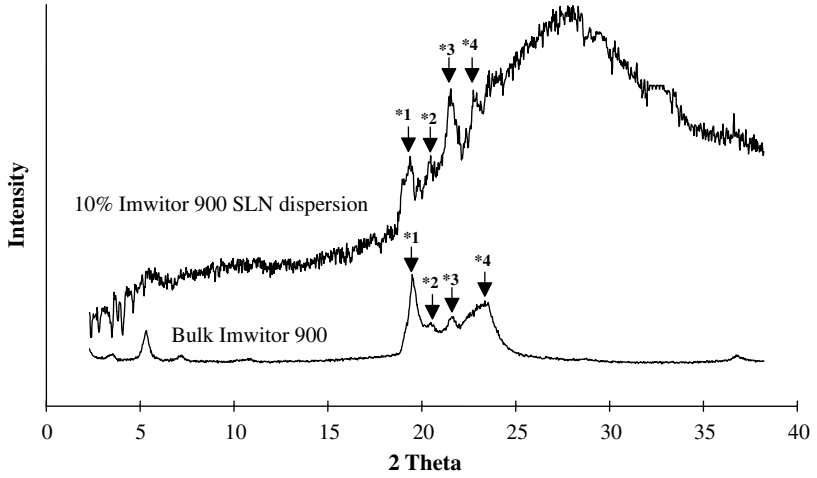

Fig. 7. WAXS scattering diagrams of bulk Imwitor®900 (lower) versus 10% drug-free Imwitor 900 SLN dispersion (analysed one day after preparation). The scattering peaks *1–*4 are the typical scattering peaks for a β′-modification. The broad reflection with a maximum around $2\theta = 28°$ is caused by the water being present in the dispersion.

lipid shows the well-known scattering peaks *1–*4 typical for β′-modification. However, these peaks can also still be detected in the X-ray pattern of the dispersion, indicating that there is still β-modification present. Combining the DSC and the X-ray data, it can be concluded that a fraction of the lipid is in the α-modification (lower melting enthalpy) and another part is present in the β′-modification. This part was not detected by DSC, which can be explained by the superposition with the melting point reduction, as described in the Thompson equation. A slightly increasing fraction of β′-modification occurs when storing, for example, CycA-loaded SLN dispersions under certain conditions (e.g., 40 °C), which can also then be detected by DSC.

The very broad reflection with a maximum around $2\theta = 28°$ of the scattering diagram of the SLN dispersion in Fig. 9 is caused by the presence of water in the sample. Evaporation of water and analysis of dry SLN does not appear sensible because water evaporation might initiate crystalline changes. Therefore, the SLN dispersion was analysed in its original composition.

3.4. Characterization of CycA-loaded SLN dispersions

SLN dispersions loaded with 10%, 15% and 20% CycA were prepared (CycA content calculated in the relation to the total particle matrix) (lipid + CycA). DSC analysis was performed with the heating rate of 5 K/min and a sample weight of 20 mg in standard aluminium pans over a temperature range of 20–85 °C (Fig. 8). A sample weight of 20 mg was selected which corresponds to 2 mg lipid in case of the investigated 10% particle dispersion. References are the bulk Imwitor®900 (Fig. 8, lower) and drug-free Imwitor®900 SLN dispersion. The DSC diagrams show a distinct shift of the peak to lower temperatures whereas a large difference between bulk lipid and SLN dispersions occurs, but less differences between drug-free SLN and drug-loaded SLN dispersions of increasing concentration up to 20%. Table 5 lists onset temperature, peak temperature and melting enthalpy. All SLN dispersions possess a distinctly reduced melting enthalpy compared to the bulk lipid (around 90 J/g versus 164 J/g). This result indicates the presence of at least a very large fraction of α-modification, in contrast to the β′-modification of the bulk lipid. In addition, CycA-loaded SLN dispersions were also analysed by WAXS. The previous section had shown that conclusions about the lipid modification cannot necessarily solely be drawn from DSC data. DSC analysis of drug-free SLN dispersions supported an α-modification. X-ray analysis proved also the existence/co-existence of the β′-modification.

The WAXS scattering pattern of the SLN dispersion loaded with 20% CycA (Fig. 9, upper) indicates an α-modification of the fatty acid chains (peak *5) confirming the DSC results. It is a liquid-crystalline modification with low intermolecular binding forces in between the fatty acid chains, a high mobility of the chains allowing the incorporation of the CycA molecule in parallel to the chains. As a comparison, the scattering pattern of the drug-free SLN dispersion is plotted. The pattern shows weak but clearly visible scattering peaks of the β-modification (*1–*4) occurring already one day after preparation of the particles. This contradicts the conclusions made only on DSC data supporting the presence of pure α-modification in drug-free SLN dispersions.

Table 5
Onset temperature, melting point (=peak maximum) and melting enthalpy of the SLN dispersions and bulk Imwitor®900 from Fig. 8

DSC parameters	Imwitor®900 (bulk material)	CycA-loaded SLN			
		0%	10%	15%	20%
Onset temperature (°C)	58.1	51.1	51.2	50.2	49.5
Peak maximum (°C)	61.1	57.5	56.9	56.4	56.1
Melting enthalpy (J/g)	164.3	90.6	89.2	89.9	86.3

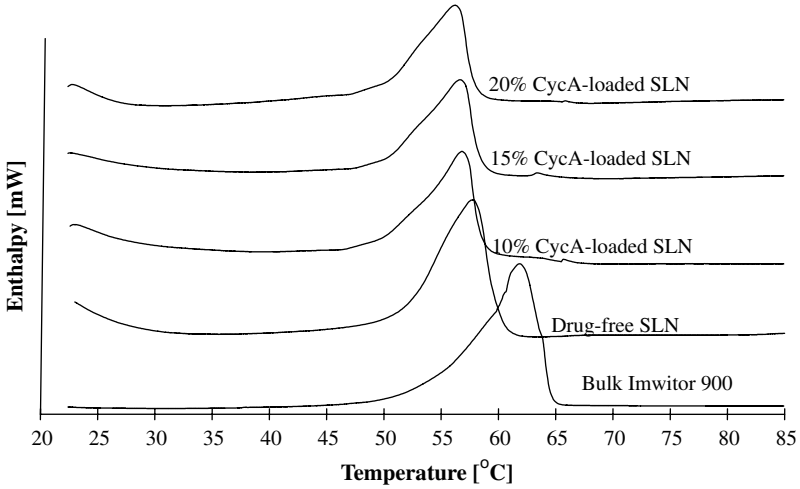

Fig. 8. DSC thermograms of cyclosporine-loaded SLN suspensions containing 10%, 15% and 20% CycA related to the particle mass. The DSC curves of drug-free Imwitor®900 SLN dispersion and bulk Imwitor®900 are given as reference. Analysis was performed one day after production.

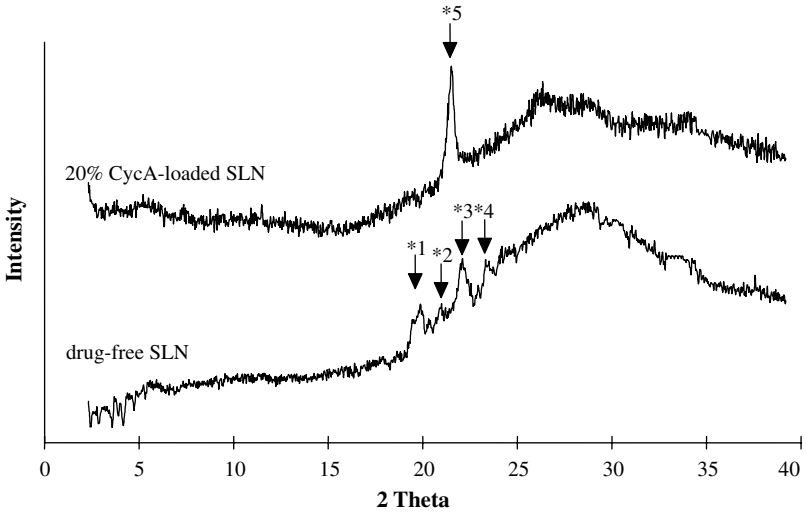

Fig. 9. WAXS scattering patterns of CycA-loaded SLN dispersion of 20% of drug in relation to particle mass (upper) and of drug-free SLN dispersion (lower). Analysis was performed one day after production. *1–*4: typical scattering peaks of β-modification; *5: characteristic scattering peak of α-modification [27]).

It is well known that SLN re-crystallize after production in higher energetic modifications. Depending on the composition of the SLN, a very fast transition to lower energy modification (e.g., β′ or β) takes place (e.g., in case of tristearin based SLN), partially a very slow transition occurs and in some cases practically no transition occurs [37,38]. The produced drug-free SLN dispersion shows already pre-formation of β′-modification one day after production (Fig. 9, lower), whereas the CycA-loaded SLN dispersion shows clearly the absence of such peaks (Fig. 9, upper). CycA seems to inhibit the transformation of the lipid to the β′-modification. This was confirmed by storing the CycA-loaded SLN over a period of 30 days [39].

A determination of *d* of the lipid lamellae – as performed for the bulk lipid – could not be realised in case of the aqueous SLN dispersions. The solid content of 10% in the aqueous surfactant phase limited the resolution of the WAXS measurements at low detection angle. To analyse the *d* a higher resolution X-ray analysis (SAXS) or synchrotron irradiation would be required [24].

The drug CycA as bulk material is partially amorphous with a certain crystalline fraction as indicated by the distinct peaks in the diffraction pattern. The bulk Imwitor®900 possesses a β′-modification as indicated by the peaks at scattering angles of about 18–25°. Processing the lipid to an aqueous SLN dispersion changes the modification to α-modification, whereas the drug-free SLN dispersion seems to transfer back to β-modification, as indicated by weak characteristic peaks. In contrast to this, the CycA-loaded SLN dispersion stays in α-modification, i.e., no peaks characteristic for the β-modification have been detected. Upon incorporation into the SLN the drug CycA loses its crystalline character, the characteristic crystalline drug peaks are not detectable anymore in the diffraction pattern of the SLN dispersion. These data in combination with the measured *d* of the bulk material support incorporation of the drug CycA in molecularly dispersed form in between the fatty acid chains of the highly mobile liquid-crystalline α-modification of the loaded SLN.

4. Conclusions

The drug CycA could be incorporated up to a relatively high loading of 20% into SLN (calculated related to the particle matrix, in case of 10% SLN dispersion this corresponds to 2% CycA in the dispersion itself). The CycA seems to be incorporated in molecularly dispersed form, i.e., as solid solution. In contrast to an o/w emulsion, the increased viscosity of the solid particle matrix in combination with the solid solution character should create a prolonged release. Release *in vivo* will take place by diffusion from the matrix and simultaneously by degradation of the lipid matrix by enzymes. Despite basic *in vitro* studies of SLN degradation by enzymes [26–28] the effect of the complex *in vivo* situation in the gut cannot be simulated, thus the degradation effect cannot be predicted. Therefore, a subsequent *in vivo* study needs to provide answers to which extent the produced CycA-loaded SLN can avoid the plasma peak and keep the plasma concentrations within the therapeutic window. Based on these *in vivo* results further optimization of the SLN formulation can be performed.

References

[1] W. Mehnert, K. Mäder, Solid lipid nanoparticles – production, characterization and applications, Adv. Drug Deliv. Rev. 47 (2001) 165–196.
[2] R.H. Müller, W. Mehnert, J.-S. Lucks, C. Schwarz, A. zur Mühlen, H. Weyhers, C. Freitas, D. Rühl, Solid lipid nanoparticles (SLN) – an alternative colloidal carrier system for controlled drug delivery, Eur. J. Pharm. Biopharm. 41 (1995) 62–69.
[3] R.H. Müller, K. Mäder, S. Gohla, Solid lipid nanoparticles (SLN) for controlled drug delivery – a review of the state of art, Eur. J. Pharm. Biopharm. 50 (2000) 161–177.

[4] E.B. Souto, R.H. Müller, Lipid nanoparticles (SLN and NLC) for drug delivery, in: A. Domb, Y. Tabata, R. Kumar (Eds.), Nanoparticles for Pharmaceutical Applications, American Scientific Publishers, 2006, pp. 103–122 (Chapter 5).
[5] Müller, R.H., Lippacher, A., Gohla, S., Solid lipid nanoparticles (SLN) as carrier system for the controlled release of drugs, in: D. Wise (Ed.), Handbook of Pharmaceutical Controlled Release Technology, 2000, pp. 377–391.
[6] E.B. Souto, R.H. Müller, Lipid nanoparticles (solid lipid nanoparticles and nanostructured lipid carriers) for cosmetic, dermal and transdermal applications, in: D. Thassu, M. Deleers, Y. Pathak (Eds.), Nanoparticulate Drug Delivery Systems: Recent Trends and Emerging Technologies, CRC Press, 2007, pp. 213–233 (Chapter 14).
[7] R.H. Müller, W. Mehnert, E.B. Souto, Solid lipid nanoparticles (SLN) and nanostructured lipid carriers (NLC) for dermal delivery, in: L. Bronaugh (Ed.), Percutaneous Absorption, Marcel Dekker, Inc., New York, Basel, Hong-Kong, 2005, pp. 719–738.
[8] R.H. Müller, J.-S. Lucks, Azneistoffträger aus festen Lipidteilchen – feste Lipid Nanosphären (SLN), European Patent 0605497, Germany, 1996.
[9] R.H. Müller, K. Mäder, A. Lippacher, V. Jenning, Fest-flüssig (halbfeste) Lipidpartikel und Verfahren zur Herstellung ochkonzentrierter Lipidpartikeldispersionen, PCT application PCT/EP00/04565, 1998.
[10] R.H. Müller, A. Dingler, S.A. Runge, T. Schneppe, S. Gohla, Large scale production of solid lipid nanoparticles (SLN™) and nanosuspensions (DissoCubes™), in: D. Wise (Ed.), Handbook of Pharmaceutical Controlled Release Technology, Marcel Dekker Inc., New York, 2000, pp. 359–376.
[11] M.R. Gasco, Method for producing solid lipid microspheres having a narrow size distribution, US Patent 5 250 236, Italy, 1993.
[12] M.R. Gasco, Solid lipid nanospheres from warm micro-emulsions, Pharm. Tech. Eur. 9 (1997) 52–58.
[13] M.R. Gasco, Solid lipid nanoparticles for drug delivery, Pharm. Tech. Eur. 13 (2001) 32–42.
[14] B. Sjöström, B. Bergenståhl, Preparation of submicron drug particles in lecithin-stabilized o/w emulsions. I. Model studies of the precipitation of cholesteryl acetate, Int. J. Pharm. 88 (1992) 53–62.
[15] M.A. Schubert, C.C. Müller-Goymann, Solvent injection as a new approach for manufacturing lipid nanoparticles - evaluation of the method and process parameters, Eur. J. Pharm. Biopharm. 55 (2003) 125–131.
[16] P. Shahgaldian, J. Gualbert, K. Äissa, A.W. Coleman, A study of the freeze-drying conditions of calixarene based solid lipid nanoparticles, Eur. J. Pharm. Biopharm. 55 (2003) 181–184.
[17] M. Trotta, F. Debernardi, O. Caputo, Preparation of solid lipid nanoparticles by a solvent emulsification–diffusion technique, Int. J. Pharm. 257 (2003) 153–160.
[18] A. Dingler, S. Gohla, Production of solid lipid nanoparticles (SLN): scaling up feasibilities, J. Microencapsul. 19 (2002) 11–16.
[19] V. Jenning, A. Lippacher, S.H. Gohla, Medium scale production of solid lipid nanoparticles (SLN) by high pressure homogenization, J. Microencapsul. 19 (2002) 1–10.
[20] J.F. Pinto, R.H. Müller, Pellets as carriers of solid lipid nanoparticles (SLN) for oral administration of drugs, Die Pharmazie 54 (1999) 506–509.
[21] A. zur Mühlen, C. Schwarz, W. Mehnert, Solid lipid nanoparticles (SLN) for controlled drug delivery – drug release and release mechanism, Eur. J. Pharm. Biopharm. 45 (1998) 149–155.
[22] K. Miyake, F. Hirayama, K. Uekama, Solubility and mass and nuclear magnetic resonance spectroscopic studies on interaction of cyclosporin A with dimethyl-α- and b-cyclodextrins in aqueous solution, J. Pharm Sci. 88 (1998) 39–45.
[23] J.H. Charuk, P.Y. Wong, R.A. Reithmeier, Differential interaction of human renal P-glycoprotein with various metabolites and analogues of cyclosporin A, Am. J. Physiol. 269 (1995) F31–F39.
[24] M.E. Lowe, The triglyceride lipases of the pancreas, J. Lipid Res. 43 (2002) 2007–2016.
[25] Penkler, L., Müller, R.H., Runge, S., Ravelli, V., Pharmaceutical cyclosporin formulation with improved biopharmaceutical properties, improved physical quality and greater stability, and method for producing said formulation, PCT application PCT/EP99/02892, 1999.
[26] R.H. Müller, S.H. Runge, V. Ravelli, W. Mehnert, E.B. Souto, Oral bioavailability of cyclosporine: solid lipid nanoparticles (SLN®) versus drug nanocrystals, Int. J. Pharm. 317 (2006) 82–89.
[27] H. Bunjes, K. Westesen, M.H.J. Koch, Crystallization tendency and polymorphic transitions in triglyceride nanoparticles, Int. J. Pharm. 129 (1996) 159–173.
[28] R.H. Müller, S. Maaßen, H. Weyhers, F. Specht, J.S. Lucks, Cytotoxicity of magnetite-loaded polylactide, polylacttide/glycolide particles and solid lipid nanoparticles, Int. J. Pharm. 138 (1996) 85–94.
[29] E. Zimmermann, E.B. Souto, R.H. Müller, Physicochemical investigations on the structure of drug-free and drug-loaded solid lipid nanoparticles (SLN™) by means of DSC and ^{1}H-NMR, Die Pharmazie 60 (2005) 508–513.
[30] M. Radtke, Nanostructured lipid carriers (NLC): Untersuchungen zur Struktur, Wirkstoffinkorporation und Stabilität, in PhD Thesis, Freie Universität Berlin, Berlin, 2003.
[31] D. Lechuga-Ballestros, A. Abdul-Fattah, C.L. Stevenson, D.B. Bennett, Properties and stability of a liquid crystal form of Cyclosporine – the first reported naturally occurring peptide that exists as a thermotropic liquid crystal, J. Pharm. Sci. 92 (2003) 1821–1831.
[32] L. Hernqvist, Crystal structures of fats and fatty acids, in: N. Garti, K. Sato (Eds.), Crystallization and Polymorphism of Fats and Fatty Acids, Marcel Dekker Inc., New York, Basel, 1988, pp. 97–137.
[33] M.M. Hassan, M.A. Al-Yahya, Cyclosporine, in: K. Florey (Ed.), Analytical Profiles of Drug Substances, Academic Press, New York, 1987, pp. 145–206.
[34] C. Schwarz, W. Mehnert, Solid lipid nanoparticles (SLN) for controlled drug delivery II. Drug incorporation and physicochemical characterization, J. Microencapsul. 16 (1999) 205–213.
[35] K. Westesen, Novel lipid based-colloidal dispersions as potential drug administration systems – expectations and reality, Colloid. Polym. Sci. 278 (2000) 608–618.
[36] K.G. Nelson, The Kelvin equation and solubility of small particles, J. Pharm. Sci. 61 (1972) 479–480.
[37] K. Westesen, H. Bunjes, M.H.J. Koch, Physicochemical characterization of lipid nanoparticles and evaluation of their drug loading capacity and sustained release potential, J. Control Release 48 (1997) 223–236.
[38] K. Westesen, B. Siekmann, M.H.J. Koch, Investigations on the physical state of lipid nanoparticles by synchroton radiation X-ray diffraction, Int. J. Pharm. 93 (1993) 189–199.
[39] S. Runge, Feste Lipidnanopartikel (SLN®) als kolloidaler Arzneistoffträger für die orale Applikation von Ciclosporin A, in PhD Thesis, Freie Universität Berlin, Berlin, 1998.